

Alma Mater Studiorum Università di Bologna  
Archivio istituzionale della ricerca

Superacid Aquivion® PFSA as an efficient catalyst for the gas phase dehydration of ethanol to ethylene in mild conditions

This is the final peer-reviewed author's accepted manuscript (postprint) of the following publication:

*Published Version:*

*Availability:*

This version is available at: <https://hdl.handle.net/11585/779386> since: 2020-11-10

*Published:*

DOI: <http://doi.org/10.1016/j.apcata.2020.117544>

*Terms of use:*

Some rights reserved. The terms and conditions for the reuse of this version of the manuscript are specified in the publishing policy. For all terms of use and more information see the publisher's website.

This item was downloaded from IRIS Università di Bologna (<https://cris.unibo.it/>).  
When citing, please refer to the published version.

(Article begins on next page)

# Superacid Aquivion® PFSA as an efficient catalyst for the gas phase dehydration of ethanol to ethylene in mild conditions.

Sara Andreoli<sup>a</sup>, Claudio Oldani<sup>b</sup>, Valentina Fiorini<sup>a</sup>, Stefano Stagni<sup>a</sup>, Giuseppe Fornasari<sup>a,\*</sup>, Stefania Albonetti<sup>a,\*</sup>

<sup>a</sup>“Toso Montanari” Department of Industrial Chemistry, University of Bologna, Bologna, 40136, Italy

<sup>b</sup>Solvay Specialty Polymers SpA, R&D Centre, Bollate (MI), 20021, Italy

\*Corresponding authors: [Giuseppe.fornasari@unibo.it](mailto:Giuseppe.fornasari@unibo.it), [stefania.albonetti@unibo.it](mailto:stefania.albonetti@unibo.it)

## Abstract

In this work, Aquivion PFSA resin was shown to be an interesting alternative as a heterogeneous catalyst for the continuous gas phase reaction of ethanol dehydration in mild conditions, thanks to its high thermal stability and superacid character. This material was confirmed to have a high thermal stability up to 300°C, after which the desulphonation process began. Under optimised reaction conditions, the Aquivion catalyst showed a conversion of over 90% ethanol as well as a selectivity to ethylene. The only detected by-product was diethyl ether, the formation of which was facilitated by low temperature. The dehydration activity was shown to depend on the number of acid sites and material shaping. Fluorescence microscopy, used to study the penetration of different alcohols into the shaped Aquivion, indicated the high polarity of ethanol, enabling the permeation into the pellet structure, thus facilitating the use of the -SO<sub>3</sub>H that is available on the resin, despite its very low surface area. The catalyst's durability was proven by a stable operation for 14 hours on-stream at 150°C, without a significant evidence of coke deposition.

**Key words:** heterogeneous acid catalysts, perfluorosulphonic resins, ethanol dehydration; ethylene

## 1. Introduction

It is widely acknowledged that there is a growing need for more environmentally acceptable processes in the chemical industry. This trend toward what has become known as ‘Green Chemistry’ necessitates a paradigmatic shift from the traditional concept of process efficiency focusing largely on chemical yield, to one that assigns economic value to the elimination of waste at the source, thus reducing pollution and avoiding the use of toxic and/or hazardous substances [1].

In this context, catalysis has played a major role, enabling reactions to become more efficient and selective, thereby eliminating large quantities of by-products and other waste compounds [2,3]. In particular, acid catalysis is by far the most important area of catalysis in all sectors of chemical manufacturing. A wide range of liquid phase industrial reactions depend on the use of inorganic or mineral acids, such as Friedel-Crafts alkylations, acylations and sulphonylations, aromatic halogenation, nitration, isomerisations, and oligomerisation [1]. These reactions are generally catalysed by mineral acids such as  $\text{H}_2\text{SO}_4$  and  $\text{HF}$ , and by Lewis acids such  $\text{AlCl}_3$  and  $\text{BF}_3$ . There has recently been considerable interest, driven by environmental and safety concerns, in finding solid alternatives for the very hazardous and corrosive mineral acid catalysts used in commercial chemical processes. Indeed, the use of solid acid catalysts presents a number of advantages, such as reduced equipment corrosion, easy product separation, less potential contamination in waste streams, and catalyst recycling [4].

Moreover, among the many different available materials, acid ion-exchange resins are one class of potential solid acid catalysts. In particular, Aquivion PFSA, a copolymer based on tetrafluoroethylene and a vinyl ether with sulphonic acid functionalities, represents a new family of perfluorosulphonic superacid (PFSA) resins with an acid strength comparable to that of pure sulphuric acid [5,6]. Thanks to its perfluorinated structure, Aquivion PFSA shows a high chemical inertness, being adaptable to a variety of reactions and resistant to strong acids, bases, and oxidative and reductive environments. Moreover, Aquivion PFSA features the shortest side chain compared to its commercially available congeners. This feature increases its crystallinity and raises the glass transition temperature to 140-150°C, permitting its use at high reaction temperature [5,7]. While this material has been widely used within the framework of fuel cells and electrolyzers [8,9] and as a catalyst for liquid phase reactions [10-16], its application as a heterogeneous catalyst in gas-phase reactions has never been investigated before.

Among the new platform molecules originating from biomass, alcohols are of considerable importance [17-23]. The dehydration of these molecules to their corresponding olefin in the gas phase is becoming an important step. Over the years, several solid acids have been developed, ranging from oxides and zeolite (working at high temperatures and suffering from deactivation) to cation exchange resins (usable only at low temperatures) [24]. Aquivion PFSA material could be a valid alternative catalyst for the reaction concerned, thanks to the higher thermal stability and superacid character.

To the best of our knowledge, no literature is available to date on the application of Aquivion as a heterogeneous catalyst in gas-phase reactions. Consequently, the aim of this work is to investigate the potential of this innovative material in the gas-phase dehydration of ethanol to ethylene.

Moreover, in this study the thermal properties of Aquivion and the penetration of alcohols into resins were examined. In particular, for the investigation of the penetration behaviour, a home-developed method exploiting fluorescence microscopy was used, leading to some interesting results. In addition, Aquivion PFSA was found to be active at a relatively low temperature and highly selective to ethylene, without showing any deactivation trend. Lastly, the influence of different reaction parameters on Aquivion PFSA catalytic activity was monitored.

## 2. Experimental

### 2.1 Materials

Aquivion-H samples were kindly provided by Solvay Specialty Polymers in different forms and with various acid loadings. Pellet samples (2.5 mm x 2.5 mm), named P98 and P87S, displayed an acid loading of 1.00 and 1.15 mmol<sub>SO<sub>3</sub>H</sub>/g, respectively. The mP98 sample was in the form of micropellets (<1 mm) and showed a 1.00 mmol<sub>SO<sub>3</sub>H</sub>/g acid loading.

With regard to the powder form, four samples with increasing acid loading were used in this work: PW98S and PW98 (1.00 mmol<sub>SO<sub>3</sub>H</sub>/g), PW87S (1.15 mmol<sub>SO<sub>3</sub>H</sub>/g), PW79S (1.25 mmol<sub>SO<sub>3</sub>H</sub>/g), and PW65S (1.48 mmol<sub>SO<sub>3</sub>H</sub>/g). On the samples labelled with S, a stabilisation treatment, consisting of exposing the resins to gaseous fluorine at a high temperature, was performed in order to end-cap the carboxylic acid groups (formed on the polymer backbone through a well-known side reaction during polymerisation) by transformation into –CF<sub>3</sub> groups [25]. The effect of the catalyst form was investigated using non-treated resins (P98, mP98, and PW98), while the influence of catalyst acidity was studied on the stabilised powders (PW98S, PW87S, PW79S, and PW65S).

Nafion® NR50, with an ion exchange capacity higher than 0.8 mmol<sub>SO<sub>3</sub>H</sub>/g, was purchased from Sigma Aldrich. Amberlyst 70 (ion exchange capacity higher than 2.55 mmol<sub>SO<sub>3</sub>H</sub>/g) was kindly provided by Solvay Specialty Polymers. The Aquivion samples studied are listed in Table 1.

Sample	Acid Loading (mmol <sub>SO<sub>3</sub>H</sub> /g)	Form
P98	1	Pellets 2.5x2.5 mm
P87S	1.15	Pellets 2.5x2.5 mm
mP98	1	Micropellets
PW98	1	Powder
PW98S	1	Stabilised Powder

PW87S	1.15	Stabilised Powder
PW79S	1.25	Stabilised Powder
PW65S	1.48	Stabilised Powder

**Table 1** Properties of the Aquivion samples used in this study.

## 2.2 Characterisation

### Thermal behaviour

The thermal behaviour of Aquivion PFSA was monitored through thermogravimetric analyses performed in a TA Instrument Q600 coupled with an FT-IR spectrometer for analysing the decomposition products. The analysis was performed by heating the powder samples from RT to 800°C, 10°C/min under air flow, and then keeping them at 800°C for 5 minutes.

### Evaluation of the **penetration** between Aquivion PFSA and alcohol.

The penetration properties of Aquivion PFSA were investigated using an innovative method based on fluorescence microscopy. For the sample preparation, Aquivion pellets (P87-S) were impregnated with a solution of fluorescein (from Sigma Aldrich) dissolved in solvents with different polarity. 7 g of Aquivion pellets were stirred in a beaker containing 15.4 g of solvent and 1.4 g of  $1.4 \times 10^{-4}$  M fluorescein in ethanol solution. The solvents used for this study were ethanol, 1-propanol, 1-butanol, toluene, dichlorometane, and cyclohexane, purchased from Sigma Aldrich. During impregnation, many samplings were performed in order to follow the evolution of the diffusion in parallel with the time of impregnation (0, 5, 10, 15, 30 minutes and 1, 2, 3, 5 hours). Fluorescence microscopy analyses were performed, using a Zeiss LSM 710 confocal microscope equipped with a 405 nm laser source and different lenses (10x, 20x, and 50x), on the external surface and the section of the impregnated pellet.

### Porosimetric measurements

The textural properties of the Aquivion samples were measured from N<sub>2</sub> adsorption-desorption isotherms at 77 K on a Micromeritics ASAP 2020 surface area analyser. Samples were first outgassed for 30 min at 100°C and 15 µmHg, and then heated for 30 min at 100°C. Specific surface area values were obtained by multi-point BET equation.

## 2.3 Catalytic tests

The catalytic behaviour of Aquivion samples, which had different forms and various acid loadings, was investigated in the gas-phase dehydration of ethanol to ethylene. The catalytic tests were carried out in a laboratory-scale system equipped with a syringe pump for ethanol feeding, gas flow meters, and a glass fixed-bed down-flow reactor with an internal diameter of 15mm (see scheme in S1). The catalyst was placed in the isothermal area of the reactor on a fritted glass plate, without diluent, and pre-treated at 150°C (1h) in nitrogen (40ml/min) to eliminate any trace of water from the material. A layer of glass beads was placed on the bed to ensure the homogeneous mixing and preheating of the gas mixture before contact with the catalyst. The catalyst performance was determined at atmospheric pressure and at a temperature ranging between 150 and 200°C, with a feeding stream of 1 % v/v of ethanol in dry helium (40 ml/min). The reaction products were detected on-line with a TCD-gas-chromatograph apparatus equipped with a CP-Sil 5 CB column (30m x 0.53mm x 0.70 mm) and maintained at 40°C during the analysis. The calculated carbon balances, if not otherwise indicated, were 99± 5 %.

### **3. Results and discussion**

#### **3.1 Aquivion PFSA thermal properties**

The thermal degradation of Aquivion PFSA powder was monitored with a TG analysis coupled with a FT-IR spectrometer. The Aquivion resin showed a significant weight loss between 300 and 520°C, with a TG profile similar to that observed by Fang et al. [26] for similar materials. From the TG-DTG profiles displayed in **Figure 1**, Aquivion PFSA appeared to decompose in three stages, starting at around 300°C.

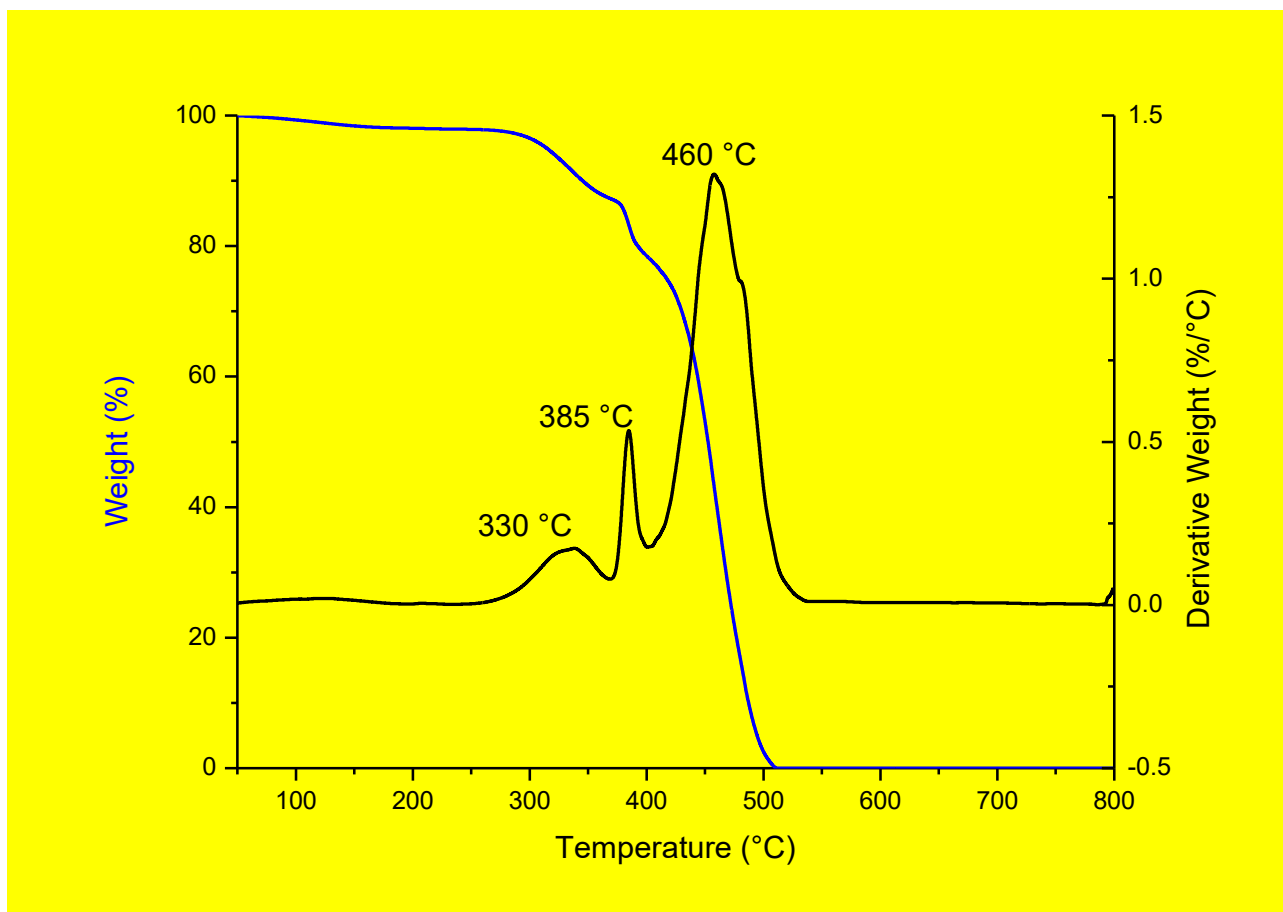


**Figure 1.** TG-DTG profiles of Aquivion powder PW98.

The slight weight loss of around 3% on heating from RT to around 300°C might be attributable to the loss of water molecules. Water was probably present due to the fact that Aquivion is quite hygroscopic. The first step, from 300 to 360°C, might be attributed to the desulphonation process, while the second one (360-400°C) might be due to the side-chain decomposition [27]. The last step, from 400 to 520°C, could be related to the PTFE backbone decomposition. Gases evolving from the material during the TG analysis were monitored by a FT-IR spectrometer. This integrated system was able to display gas component evolution profiles at the same time as the TG weight loss. The spectra obtained during each decomposition step are shown in **Figure 2**.

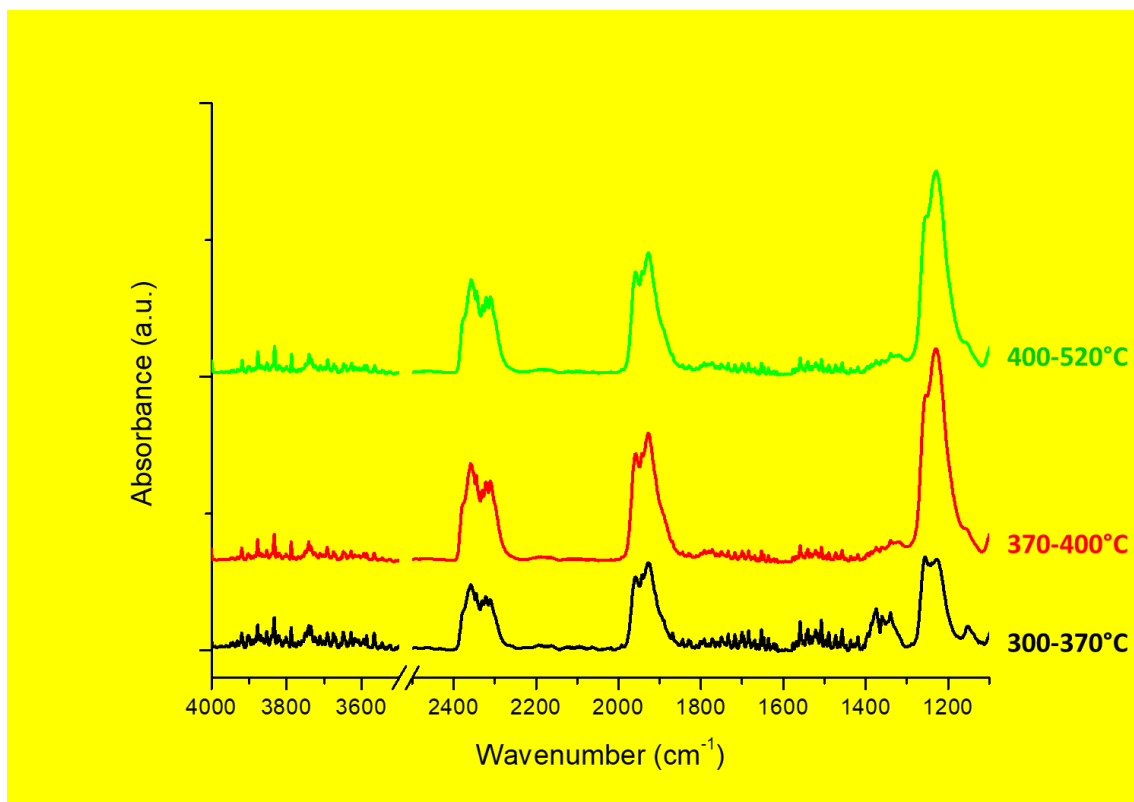


**Figure 2.** FT-IR spectra of the gas-phase degradation products released during the three main losses of weight (Aquivion PW98).

During the degradation of Aquivion, mainly  $\text{SO}_2$ ,  $\text{CO}_2$ , HF, carbonyl fluorides, and fluorocarbons were produced.

In the FT-IR spectra acquired during the first decomposition step (300-370°C), a number of different bands can be observed. In the 3800-3500  $\text{cm}^{-1}$  region, the major absorbance is due to water and HF [28]. The double band at 2359 and 2311  $\text{cm}^{-1}$  can be attributed to  $\text{CO}_2$ , which may be formed following a mechanism suggested by Wilkie et al. [29]. The author studied the degradation of Nafion in nitrogen atmosphere and hypothesised that an initial loss of water from the sulphonic acid produced anhydride which, in turn, might have reacted with another sulphonic acid to produce a sulphonate ester. Then, the reaction between this ester and water produced a carboxylic acid that could undergo decarboxylation, producing  $\text{CO}_2$ . These considerations may also be made for Aquivion degradation in air atmosphere, because it has been demonstrated that the presence of oxygen did not have a great effect on the material stability and, therefore, on the way it decomposed [30].

During this decomposition step, substituted carbonyl fluorides (RCOF) were also released, based on the bands [29] at 1957 and 1916  $\text{cm}^{-1}$ . The band at 1333  $\text{cm}^{-1}$  may be attributed to  $\text{SO}_2$  [29,31]. This signal totally disappeared in the spectra acquired during the following decomposition steps, confirming that the first step consisted of a desulphonation process and that at higher temperatures



the amount of SO<sub>2</sub> decreased dramatically, as observed also by Wilkie et al. [29]. Indeed, the bond initially broken was the C-S bond, giving a carbon-based radical and a SO<sub>3</sub>H radical, which cleaved to produce SO<sub>2</sub> and a hydroxyl radical.

Perfluoro compounds showed several C-F stretching peaks over the broad range 1400-1000 cm<sup>-1</sup> [31], including an intense peak around 1260 cm<sup>-1</sup>, which could also be due to an asymmetric stretching in the SO<sub>2</sub>-OH group. This intense peak was also observed at higher temperature and it is unlikely that R-SO<sub>2</sub>-OH species could exist in a gas phase at temperatures around 400°C. Consequently, this band was mainly due to C-F fragments.

As for the spectra acquired during the second and third decomposition steps, they are very similar, and the greatest absorbances are due to HF, substituted carbonyl fluorides, and C-F stretching vibration, while the SO<sub>2</sub> band is nearly absent.

In the same system and conditions, the thermal properties of the Aquivion powder, which is characterised by different acid loading (1.15 mmol<sub>SO3H</sub>/g for PW87-S and 1.25 mmol<sub>SO3H</sub>/g for PW79-S), were also investigated and compared with the PW98 sample, as shown in **Figure 3**.

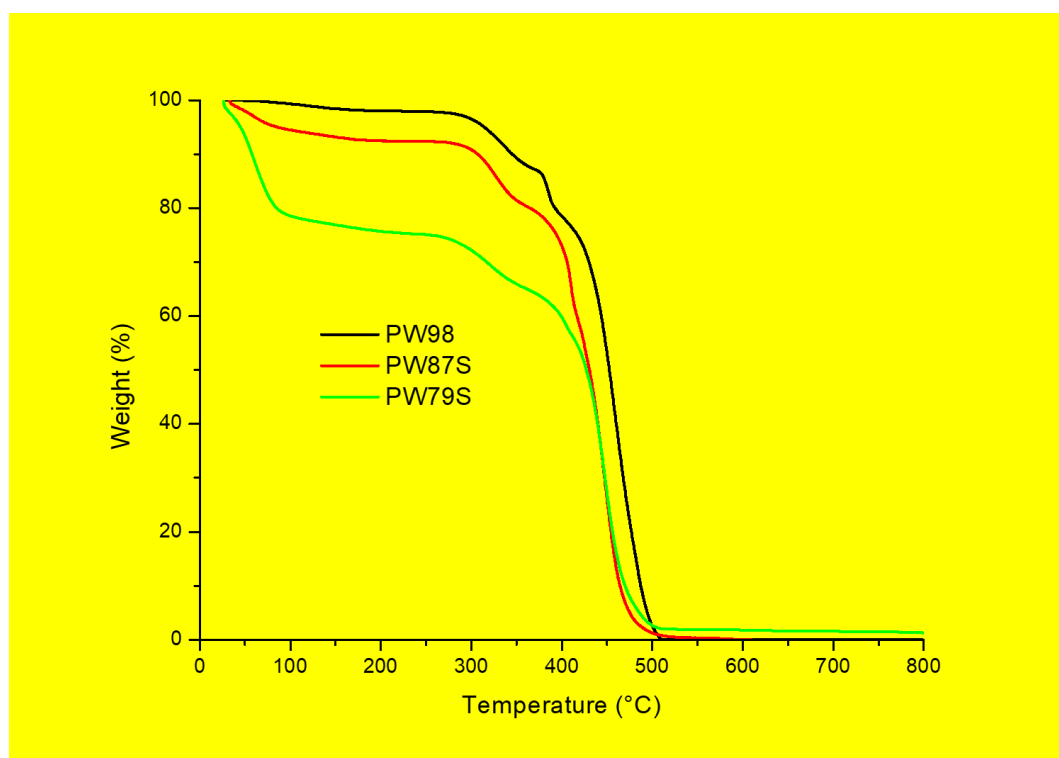


**Figure 3.** TG profiles of Aquivion PW98 (black), PW87S (red) and PW79S (green).

TG profiles clearly evidenced a trend of the acid loading, with weight loss taking place under 200°C, due to the moisture content. Indeed, the higher the acid loading, the greater the weight loss. The most acidic sample (PW79-S) showed a 20% initial weight loss, due to its higher acid loading, which led to a greater affinity with water moisture. The samples with a low acidity showed a reduced moisture loss: 7% for PW87S and 3% for PW98. The degree of hydration of the Aquivion

samples with the acid loading is confirmed by the ATR analysis, as reported in Figure S2 with the corresponding band attribution [32]. The higher the acid loading, the greater the amount of water, as the bands related to the –OH stretching and bending show.

Air-TGA was also performed on the Aquivion PW98 in the ammonium form. The aim of this experiment was to discover the strength of the –SO<sub>3</sub>H acid group; if the acid resin is put in contact with a basic solution such as ammonia solution, salt – in particular ammonium salt – may form. With a weak acidity, NH<sub>3</sub> should be released at a low temperature through the decomposition of ammonium salt; conversely, in the presence of strong acid groups, NH<sub>3</sub> should be released at a high temperature. During the thermogravimetric analysis, the compounds released were the same as in other samples, but ammonia was not detected by the FT-IR spectrometer. This was probably because the NH<sub>3</sub> concentration was too low. Some differences can be observed in TGA/DTG profiles when comparing the sample in the ammonium form with the original one. In particular, the first and the second weight loss are visibly shifted to higher temperatures for the sample in the ammonium form. This is probably due to a higher stability of the salt form, Figure S3.

### 3.2 Evaluation of Aquivion PFSA penetration with alcohols

The swelling phenomena due to solvent sorption could be of particular importance in the use of resins such as PFSA as catalysts [33]. A dry resin with a very small surface area can swell when brought into contact with a solvent; Aquivion PFSA was demonstrated to swell in n-dodecanol to a large extent, especially in the powder form [16]. Moreover, with PFSA, when a solvate such as water diffuses into the resin, it can interact with its sulphonic acid sites and can form protonated water molecules that further extend the penetration phenomena [34]. The solvent swelling can create space inside the resin and make it possible for small molecules to get access to the polymer network.

This effect is mainly observed in liquid phase reactions, but an effect on gas-phase reactions – in low temperature conditions as in our case – cannot be excluded. Indeed, a significant improvement of Nafion-based catalyst performances in the gas phase dehydration of C6 alcohols has been reported [35], due to the swelling of the polymeric matrix caused by the water produced in the dehydration step.

Since the shaping of Aquivion PFSA into pellets was demonstrated to significantly reduce its swelling ability [16] we decided to study the behaviour of Aquivion pellets in the presence of different alcohols (ethanol, 1-propanol, 1-butanol) by adding fluorescein as a luminescent marker to the various solvents. In this way, it was possible to track the uptake of fluorescein-containing solvents through the pellet section in relation to the time of impregnation.

The penetration of the solvents into the resin was found to be strongly dependent on the impregnation time and solvent polarity (Table 2), as also observed by other authors [37,38]. As a rule, the penetration of the solvent into the polymer network was more effective as the polarity of the solvent increased. In Figure 4a, the fluorescence microscopy images of the pellets that were obtained after their exposition to fluorescein-labelled ethanol at progressive impregnation times are shown.

Solvent	$E_T^N$ (from ref. 36)
Ethanol	5.2
1-Propanol	4.3
1-butanol	4.0
Toluene	3.1
Dichloromethane	2.4
Cyclohexane	0.2

**Table 2.** Empirical solvent polarity of the solvents used in penetration tests.

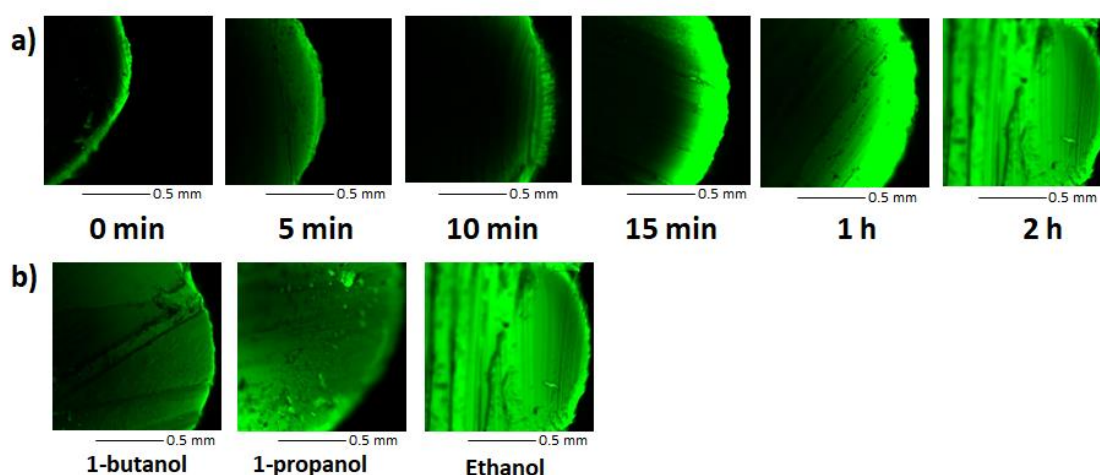


**Figure 4.** Fluorescence microscopy images of a P87S pellet section with different impregnation times using ethanol a), and different solvents at 2h of impregnation b).

All the acquired images clearly show the increasing penetration of ethanol as the impregnation time is prolonged, with a P87S pellet section completely fluorescent after 2 hours. For shorter periods (5 and 10 minutes), fluorescein was detected only on the external surface of the pellet, while after 15 minutes, fluorescein began to permeate into the core. A similar trend was also observed in the case of impregnation with other alcohols such as 1-propanol and 1-butanol. However, the extent to which penetration occurred appeared markedly dependant on the polarity of alcohol solvents (**Figure 4b**). Indeed, after 2 hours of impregnation, only the pellet impregnated with ethanol was completely fluorescent, whereas fluorescence was less evident in the presence of the less polar 1-propanol and 1-butanol.

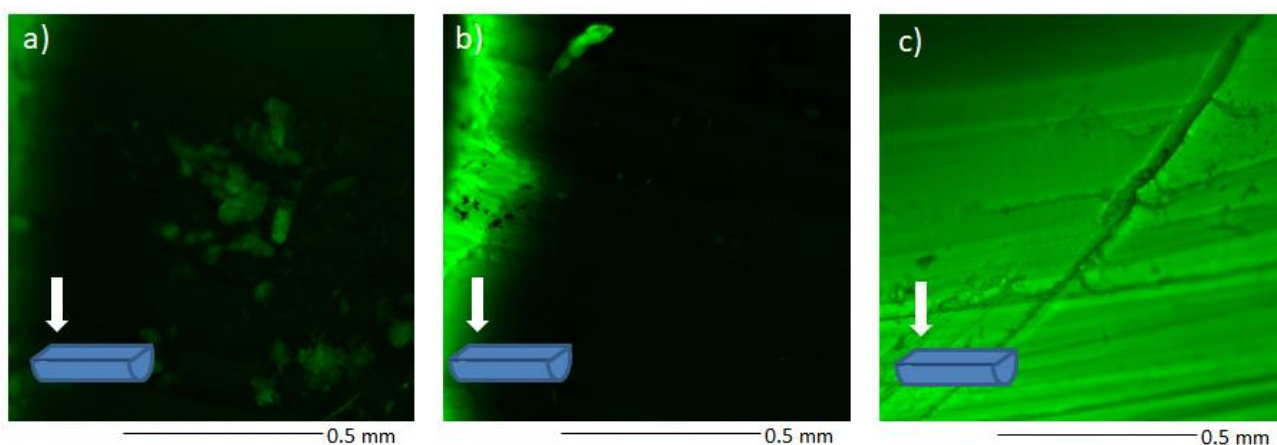


**Figure 5.** Comparison of the fluorescence images of P87-S pellet section impregnated with cyclohexane ( $E_T^N=0.2$ ) a), dichloromethane ( $E_T^N=2.4$ ) b) and toluene ( $E_T^N=3.1$ ) c) at 3h of impregnation.

In the presence of intermediate-polar and non-polar aprotic solvents (toluene, dichloromethane, cyclohexane), fluorescein did not readily permeate the pellet. Indeed, only after 3 hours of impregnation with fluorescein-labelled toluene (**Figure 5**) did the pellet become completely fluorescent. In the case of dichloromethane and cyclohexane, the penetration was almost negligible, again suggesting the importance played by the polarity of the solvent. These data indicate that, in an initial approximation, ethanol could partially permeate the pellet structure during the tests in a continuous flow, thus accessing the different acid sites present on the materials and allowing the better use of the  $-\text{SO}_3\text{H}$  which is available on the resin.

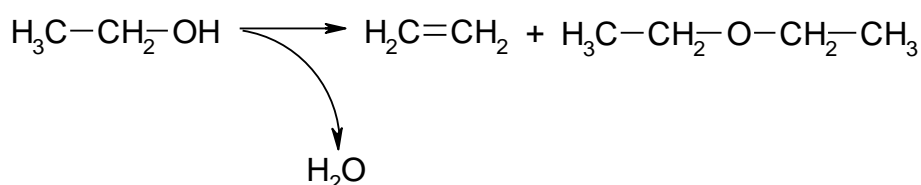
### 3.3 Aquivion textural properties

$\text{N}_2$  adsorption/desorption analyses showed very small surface area values ( $0.2\text{-}0.3\text{ m}^2/\text{g}$ ) for all the Aquivion samples, both in powder and pellet form. During the analyses, the swelling took place in the presence of condensed nitrogen, giving the adsorption and desorption isotherms different shapes (**Figure S4**). As a matter of fact, for each sample, the adsorption and desorption isotherms do not

overlap. This effect was particularly evident in the low pressure region, suggesting a material modification by nitrogen adsorption through swelling phenomena.

### 3.4 Aquivion catalytic activity

Aquivion was tested as a heterogeneous catalyst in a continuous gas-phase process for the dehydration of ethanol. In this reaction (**Scheme 1**), the main products detected were ethylene and diethyl ether (DEE). Acetaldehyde formation, which could be observed in this reaction, is an endothermic process which is facilitated by high temperatures. Since the temperature studied was below 200°C, this molecule was never observed in our study.



**Scheme 1.** Ethanol dehydration to ethylene and diethyl ether (DEE).

Many parameters were studied in order to optimise the reaction and evaluate the influence of resin properties on the catalytic activity.

#### *Effect of the reaction temperature*

The dehydration of ethanol to ethylene was first studied based on the reaction temperature over the pellet and powder forms of Aquivion. **Figure 6** shows the catalytic behaviour of the pellet form of P98 at 150, 180, and 200°C.

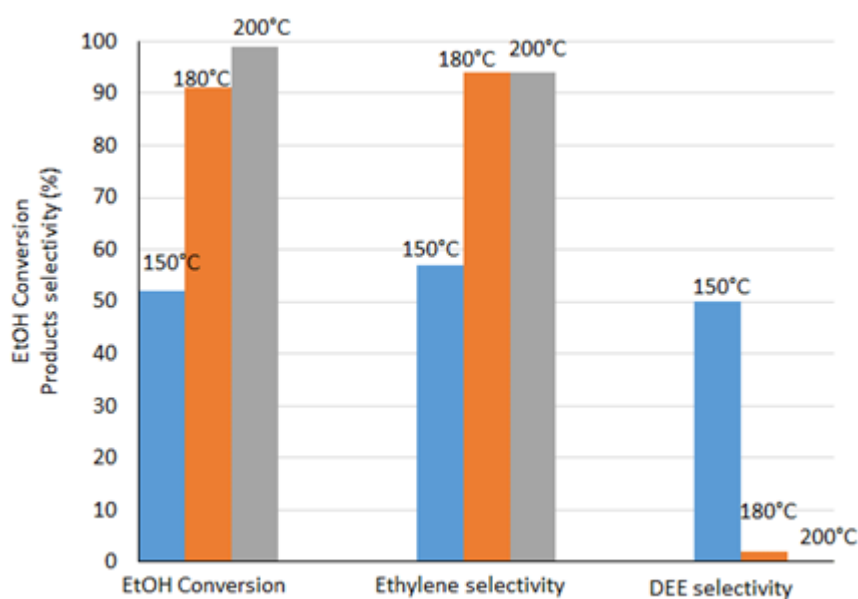


**Figure 6.** Trend of the catalytic activity of Aquivion P98 with reaction temperature. Test conditions:  $m_{\text{cat}}=0.65\text{g}$ ,  $\tau=1\text{s}$ , EtOH 1% v/v.

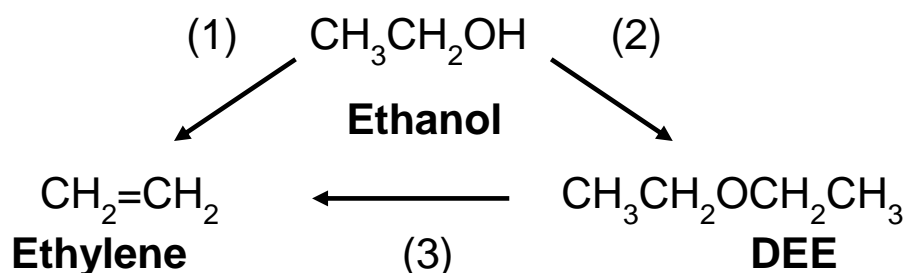
First, it should be stressed that Aquivion showed interesting catalytic properties, being active in ethanol dehydration at relatively low temperatures. Moreover, at 200°C Aquivion provided an almost complete ethanol conversion with a very high selectivity to ethylene. As the temperature increased, ethanol conversion and ethylene selectivity increased, while DEE (diethyl ether) selectivity decreased. Ethanol conversion rose from 50% at 150°C up to near 100% at 200°C. With an increasing reaction temperature, ethylene selectivity shifted from 55% at 150°C to more than 90% at 200°C. DEE selectivity from less than 50% at 150°C decreased to 0% at 200°C, while the carbon balance decreased slightly when the reaction temperature increased.

Similar results and trends were also observed for Aquivion P87S and all Aquivion powders with different acid loadings, thus confirming previously reported results obtained using different kinds of acidic catalysts such as zeolites [39], rare earth phosphates [40], and heteropolyacids [41] at higher temperatures. The general mechanism shown by these materials demonstrated that DEE formation is the result of a condensation reaction between two ethanol molecules – an exothermic process penalised by temperature increases – while ethylene is formed via the endothermic dehydration reaction facilitated by higher temperatures.

It is well known that the transformation of ethanol to ethylene over an acidic catalyst may follow parallel and consecutive routes and that many different parameters, such as the type of catalysts, its surface acidity, and the reaction conditions, affect the preferred reaction route [42,43].

Phung et al. [44,45] demonstrated that ethanol dehydration to DEE using strong Brønsted acidic material occurs selectively at low temperatures with a “bimolecular” mechanism involving the

reaction of ethoxy groups with undissociated ethanol, while dehydration to ethylene occurs selectively at high temperatures with an elimination mechanism, but also, at low temperatures, with a consecutive path via DEE formation and cracking (Scheme 2).



**Scheme 2.** Ethanol dehydration to ethylene and diethyl ether (DEE).

The trend of ethylene and DEE selectivity depending on space velocity in our study is similar to what was previously observed [45,46] and suggests, also in the presence of Aquivion, the formation of some ethylene at high contact time, due to the consecutive cracking mechanism on the produced DEE (Scheme 2 - reaction 3).

As reported in Figure 6, the formation of DEE from ethanol (reaction 2) is facilitated at low temperature and – being bimolecular and with a high reaction order – by low conversions. On the contrary, the direct formation of ethylene becomes predominant in high temperature and high conversion conditions. Phung et al. [44] suggest that the reaction forming ethylene has a high temperature dependence, i.e. a higher activation energy than that of DDE formation. The trends observed confirm the mechanism proposed by Phung et al. [45] which follows two paths: one direct, i.e. the dehydration of ethanol to ethylene, and one consecutive, in which DDE formation and subsequent cracking on acid sites take place.

The effect of cracking shown by Aquivion may be due to the high acid strength of Bronsted, thus confirming what was reported by Phung et al. [45]: Bronsted's strong acidity facilitates both ethanol dehydration and DDE cracking. The high acidity makes it possible to obtain a high activity at low temperatures; however, it is also conducive to the formation of by-products such as oligomers and longer olefins, as well as of coke [46]. This may explain the slightly decreased carbon balance in conditions of high temperature and high contact times.

### *Effect of the space velocity*

The effect of the space velocity was investigated over the Aquivion pellet P98 at 150°C. Ethanol conversion depends significantly on this parameter. Indeed, the lower the space velocity (higher contact time), the greater the ethanol conversion (**Figure 7**).

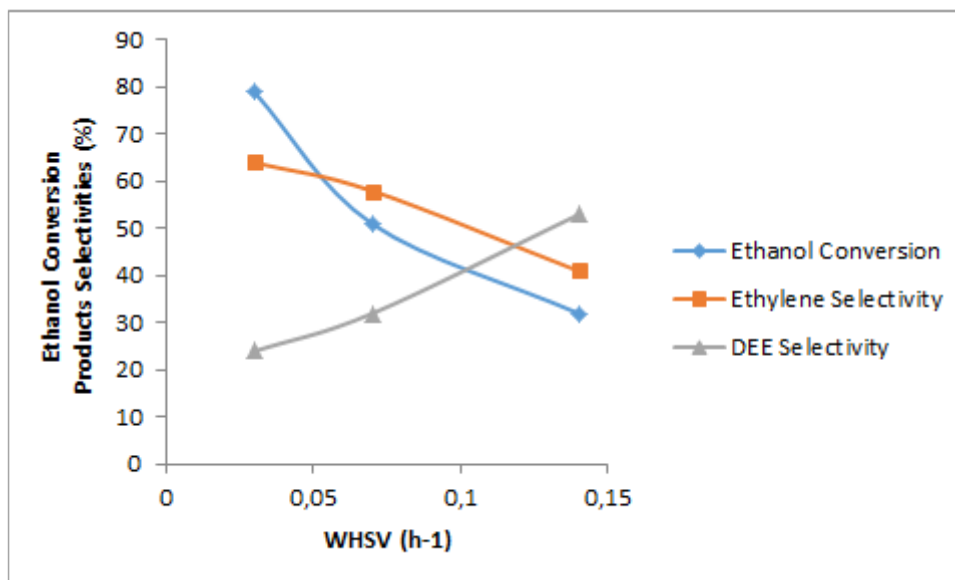


**Figure 7.** Ethanol conversion, ethylene selectivity and DEE selectivity on Aquivion P98 at 150°C depending on weight hourly space velocity (WHSV).

Ethylene selectivity decreases as space velocity increases, while DEE selectivity clearly has a reverse trend since, at lower space velocities, it falls to the advantage of ethylene selectivity.

These data provide information for several speculative considerations on the reaction mechanism involved in the dehydration of ethanol under the reported conditions.

**Effect of the catalyst form.** The influence of the catalyst form on catalytic performances in the continuous gas-phase reaction was studied on the Aquivion catalysts in the form of pellets (P98), micropellets (mP98), and powder (PW98), all with the same acid loading. It is important to point out that, in an industrial perspective, resin cannot be used in powder form, while the impact of shaping Aquivion on catalytic performances was already demonstrated to be an important parameter to be taken into account for the implementation of large-scale processes in the liquid phase [16]. Each catalytic test was performed with the same catalyst amount and contact time in order to rule out possible effects due to these parameters. The effect of the catalyst form on ethanol conversion and products yields is summarised in **Figure 8**.



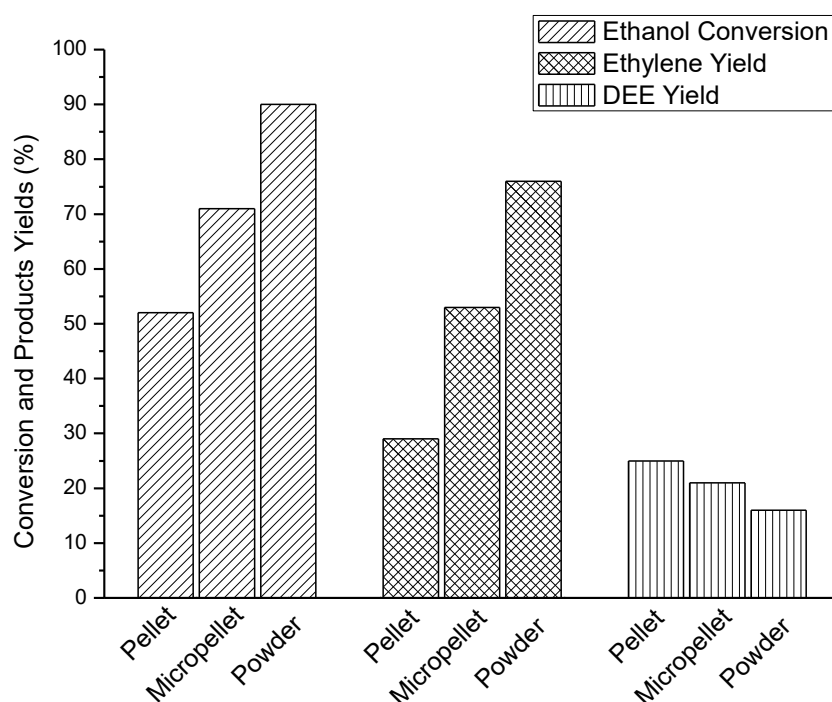


**Figure 8.** Trend of the catalytic activity with catalyst form: pellet (P98), micropellet (mP98), and powder (PW98). Test conditions:  $m_{\text{cat}}=0.7\text{g}$ ,  $\tau=1\text{s}$ , EtOH 1% v/v,  $T=150^{\circ}\text{C}$ .

The catalyst form seems to have a great effect on catalytic performance using Aquivion in continuous gas-phase reactions, as also observed in liquid-phase reactions [16]. When the catalyst particle size was decreased, ethanol conversion and ethylene yield increased, while DEE yield decreased. Indeed, ethanol conversion increased from 50% for the pellet to 90% for the powder. A significant effect can be also observed on ethylene yield, which rises from 30% for the pellet to around 75% for the powder. DEE yield decrease is less evident, falling from around 25% for the pellet to 15% for the powder.

This trend is probably due to the different availability of the active surface when changing the catalyst form. Aquivion has very low surface area values for all the samples, and acid sites prove to be inaccessible or poorly accessible. The powder ensured a greater accessibility of the active sites compared to the micropellet and pellet forms. However, it has been demonstrated that Nafion-based catalysts have a low catalytic activity in gas phase reactions using non-polar reactants – due to the difficult accessibility of acid sites in the absence of swelling in the polymeric framework [35]. Nevertheless, when polar molecules are present in the reaction (such as the water produced in the dehydration step of C6 alcohols), a significant improvement in the catalytic performance was observed due to the gradual swelling of the polymeric matrix caused by water. Fluorescence tests on Aquivion indicate that ethanol is also able to permeate the structure of the pellet, thus making

accessible sites which, otherwise, would not be available for the reaction in gas phase, and enabling good ethanol conversions.

**Effect of the acid loading.** Aquivion powders with different sulphonic loadings – 1.0, 1.15, and 1.48 mmolSO<sub>3</sub>H/g – were used to study the effect of the acid loading on the catalytic performance. Catalytic tests were performed at 120°C with a constant catalyst amount. The results obtained are shown in **Figure 9**.

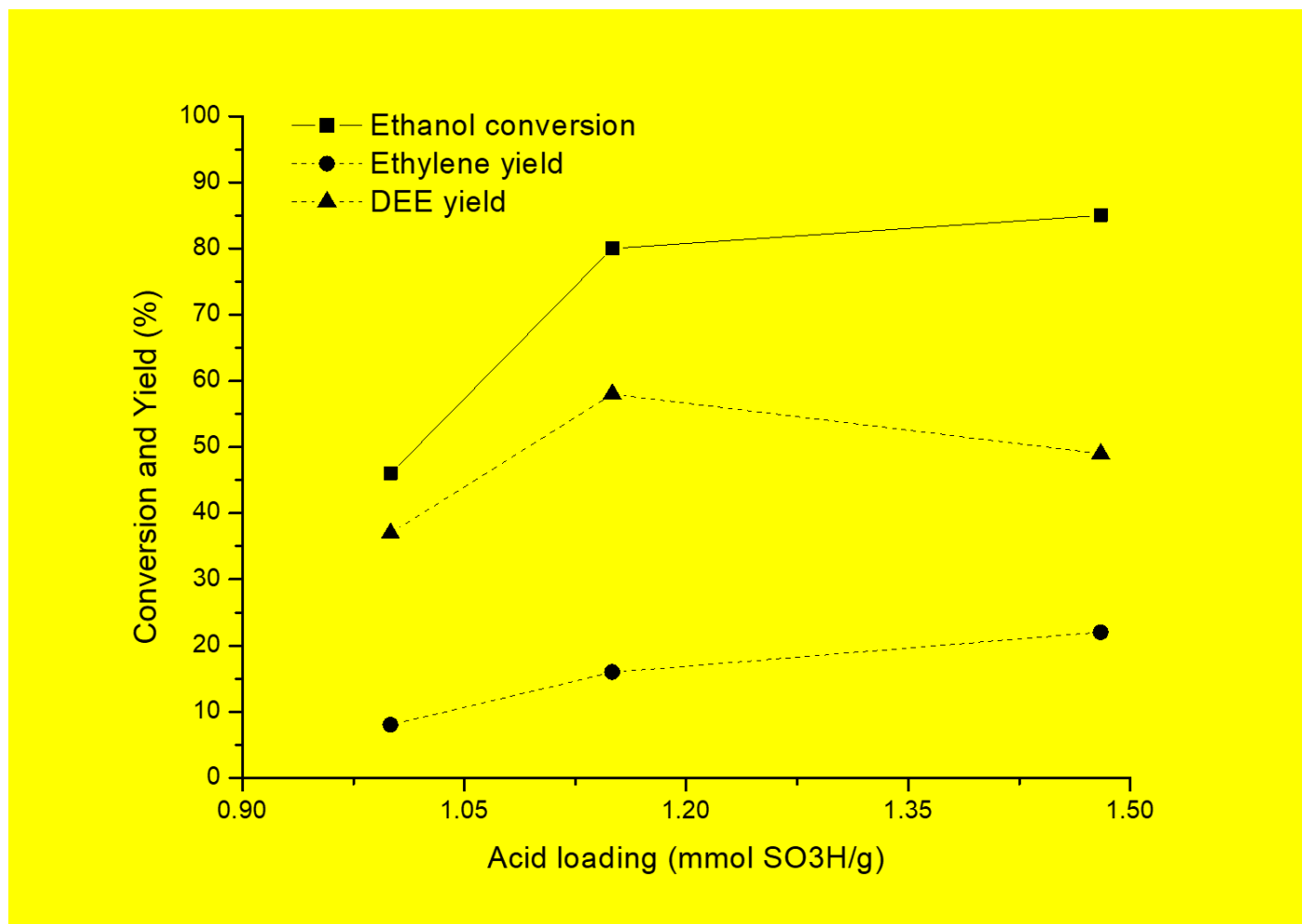


**Figure 9.** Trend of the catalytic activity at 120°C with acid loading: 1.00 (PW98S), 1.15 (PW87S) and 1.48 (PW65S) mmolSO<sub>3</sub>H/g.

When the acid loading is increased, a trend in the conversion and yields can be observed. In the case of the most acidic catalysts, ethanol conversion and ethylene yield are higher. The effect on selectivity is variable, but the formation of ethylene over DEE is always facilitated. A high acid loading also favours the formation of by-products such as oligomers and longer olefins with decreasing the carbon balance. As a general observation, increasing acidity leads to a higher ethanol

conversion, from 45 to 85%. The same trend is observed for ethylene yield, which rises from 8 to 22%.T

**Comparison with other acid catalysts.** In order to find out whether the catalytic performances of Aquivion materials were noteworthy in the field of gas-phase dehydration reactions, we tested some well-known sulphonic resins, such as Amberlyst and Nafion, in ethanol dehydration. Materials belonging to the Amberlyst family are generally sulphonic ion-exchange resins that consist of copolymers of divinylbenzene (DVB), styrene, and sulphonic acid groups [47]. The major drawbacks of polystyrene-based sulphonic resins are: (i) the acid's strength, which is considered to be relatively low (the Hammett acidity function is evaluated as  $H_0=-2.2$ ), and (ii) the limited stability temperature range (up to 150-180°C) [48]. Solutions for these substantial drawbacks are provided by perfluoropolymer ionomers, also known as the perfluorosulphonic acids family, which includes Nafion and Aquivion materials.

Amberlyst, Nafion, and Aquivion catalysts were tested in the ethanol dehydration at 150°C in pellets form and similar dimension. These catalysts display acid loading in a similar range:  $\geq 2.55$  mmol<sub>SO<sub>3</sub>H</sub>/g for Amberlyst,  $\geq 0.8$  mmol<sub>SO<sub>3</sub>H</sub>/g for Nafion, and 1.00 mmol<sub>SO<sub>3</sub>H</sub>/g for Aquivion.

**Figure 10** shows the comparison of Amberlyst (A70), Nafion (NR50), and Aquivion (P98) catalysts.

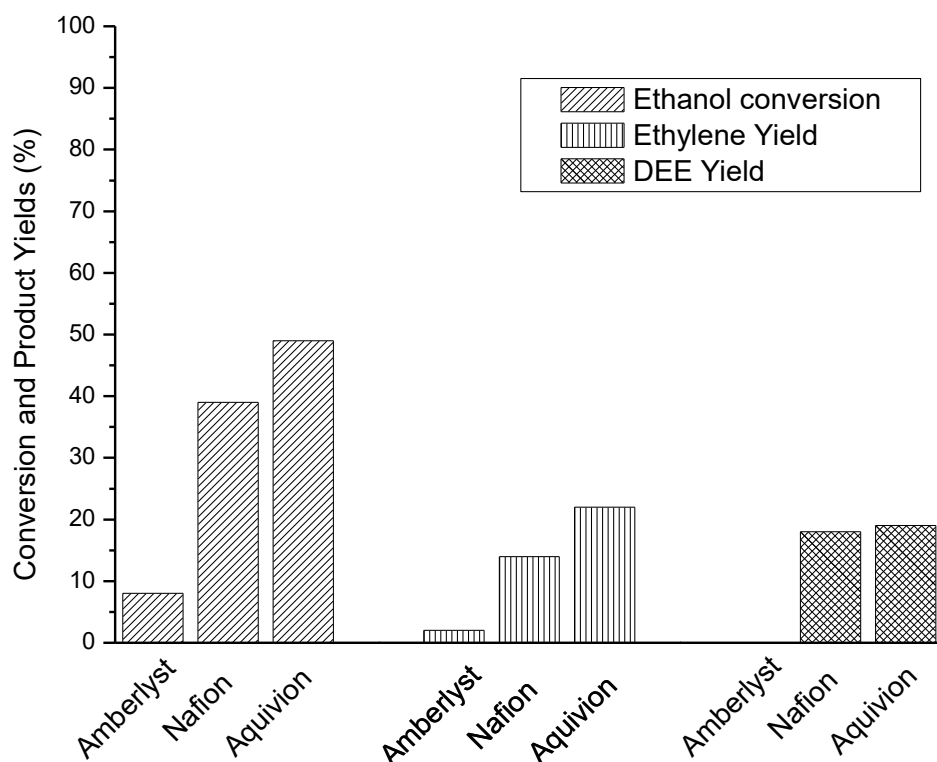


**Figure 10.** Influence of the catalyst type: Amberlyst (A70), Nafion (NR50), and Aquivion (P98). Test conditions:  $\tau=1s$ , EtOH 1% v/v,  $T=150^{\circ}C$ .

Aquivion P98 was found to be the most active, in terms of ethanol conversion and ethylene yield, followed by the Nafion and Amberlyst catalysts. Perfluorosulphonic resins gave a higher ethanol conversion (39% for Nafion and 49% for Aquivion), ethylene yield (14% for Nafion and 22% for Aquivion), and DEE yield (18% for Nafion and 20% for Aquivion) than the polystyrene-based sulphonic resin, although this shows the highest acidity among the tested catalysts. Indeed, the Amberlyst catalyst produced the lower ethanol conversion and ethylene yield; moreover, no DEE was formed. The greater catalytic activity of Aquivion and Nafion is probably due to the higher acidic strength given by the presence of fluorine, which leads to a prominent dissociation tendency of  $-SO_3H$  groups. It is generally accepted that perfluorinated resins are very strong acids with Hammett acidity function values between -11 and -13 [13, 49], thus being defined as superacid [24]. For comparison purposes, note that the Hammett acidity function for classical sulphonated polystyrenes is around -2 [6].

### ***Durability Test***

Based on the interesting results obtained from Aquivion catalysts, the durability of this material was investigated under reaction conditions. A 14-hour test was performed on the P98 catalyst, monitoring ethanol conversion and product yields (**Figure 11**).

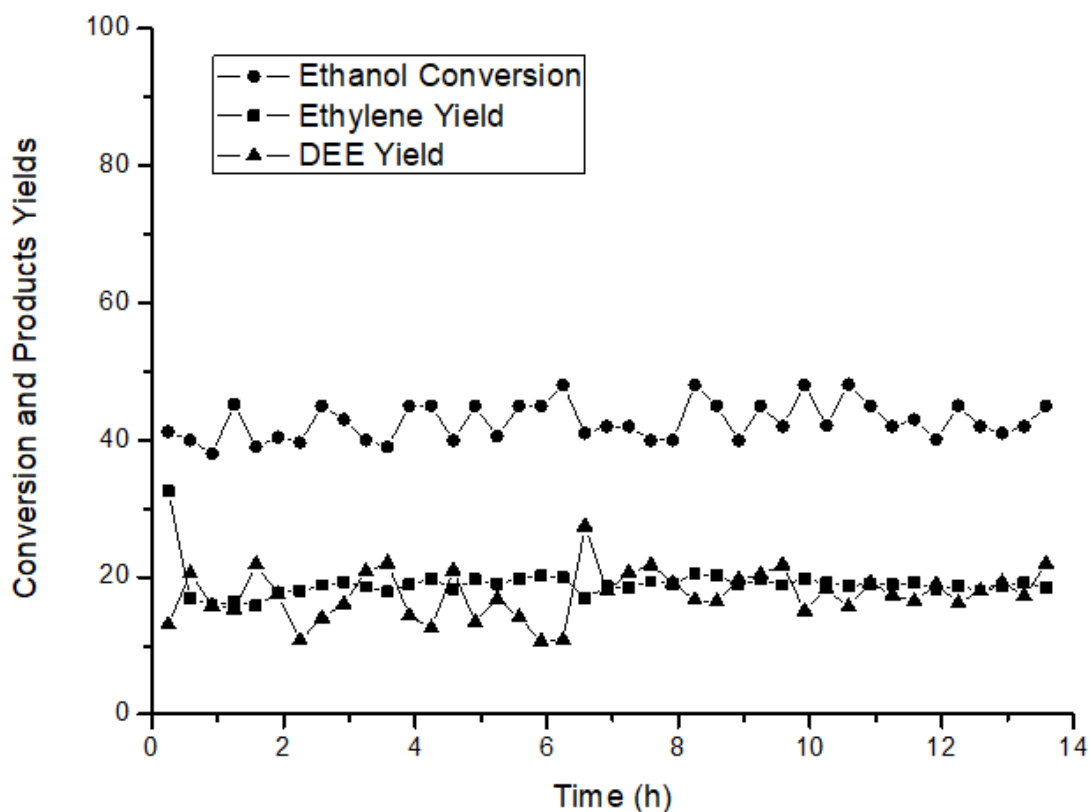


**Figure 11.** Durability test for P98. Test conditions:  $\tau=1$ s, EtOH 1% v/v,  $T=150^{\circ}\text{C}$ .

The catalyst performance at  $150^{\circ}\text{C}$  appeared to be stable with time on stream, while the material did not show any evident deactivation trend. Similar results were obtained at higher temperatures.

Despite the very good performance and durability of P98, the characterisation on the used catalyst showed some changes in the surface of the material due to different phenomena (**Figure S5**).

Indeed, on the surface of the used catalysts, some very low intensity bands typical of the aliphatic C-H in the  $2900\text{--}3000\text{ cm}^{-1}$  range) were detected, while the colour of the material turned from yellow to black when the temperature increased from  $150$  to  $200^{\circ}\text{C}$ . It was very difficult to estimate the quantities of the impurities deposited. However, the slight increase in the FTIR band and changes in the catalyst colour seen with the increase in temperature may be related to a higher quantity of the heavy compounds deposited on the surface. It must be stressed that the dark colour observed in the used catalysts is not only due to the formation of heavy compounds on the surface,

but also to the simultaneous transformation of the material itself. Indeed, the catalyst colour was modified even after the blank test, in the absence of ethanol.

## Conclusions

This paper reports that Aquivion PFSA, a perfluorosulphonic acid polymer, may be a valid heterogeneous catalyst for the gas phase reaction of ethanol dehydration. This material confirmed a high thermal stability up to 300°C, after the desulphonation process started.

The interaction with alcohols was examined by using a luminescent marker and fluorescence microscopy. The penetration of different alcohols into pellets of Aquivion was demonstrated to increase with increasing the impregnation time and polarity of the solvent. These data seem to indicate that ethanol can partially permeate inside the pellet structure during the tests in used conditions, accessing to the acid sites present in the material. Nevertheless, with decreasing the size of the particles - changing the catalyst form from pellets to grains - increased the catalytic performances. Indeed, using powder materials, the contact between ethanol and the active sites was enhanced, making accessible sites that otherwise would not be available for the reaction in gas phase and suggesting the necessity to further study the optimization of Aquivion based materials to improve the accessibility of the acidic groups.

Under very mild reaction conditions, Aquivion PFSA was found to be markedly more active in terms of ethanol conversion and ethylene yield than other acidic catalysts, due to its superacid character. Under optimized reaction conditions it showed very high ethanol conversion and selectivity to ethylene at relatively low temperature, (confirming the consecutive paths in the formation of ethylene, in which the DEE cracking takes place).

The durability of the catalyst was demonstrated by stable operation for 14 hours on stream without a deactivation trend and significant evidence of coke deposition.

## References

1. P. Gupta, S. Paul, *Catal. Today* **236** (2014) 153-170.
2. M. Lancaster, *Green Chemistry: An Introductory Text*, Royal Society of Chemistry, Cambridge, 2002.
3. P. T. Anastas, M. M. Kirchhoff, T. C. Williamson, *Appl. Catal. A: Gen.* **221** (2001) 3-13.
4. M. A. Harmer, Q. Sun, *Appl. Catal. A: Gen.* **221** (2001) 45-62.
5. L. Bianchi, E. Ballerini, M. Curini, D. Lanari, A. Marocchi, C. Oldani, L. Vaccaro, *ACS Sustainable Chem. Eng.* **3** (2015) 1873-1880.
6. G. A. Olah, G. K. S. Prakash, J. Sommer and A. Molnár, *Superacid Chemistry*, John Wiley & Sons, Inc., Hoboken, NJ, 2009.
7. R. Tassini, V. D. Rathod, S. Paganelli, E. Balliana and O. Piccolo, *J. Mol. Catal. A: Chem.*, **411** (2016) 257-263

8. C. D'Urso, C. Oldani, V. Baglio, L. Merlo, A. S. Aricò, *J. Power Sources* **272** (2014) 753-758.
9. A. Donnadio, M. Pica, S. Subianto, D. J. Jones, P. Cojocaru, M. Casciola, *ChemSusChem* **7** (2014) 2176-2184.
10. H. Shi, Z. Fan, B. Hong and M. Pera-Titus, *ChemSusChem*, **10** (2017) 3363–3367.
11. C. Moreno-Marrodan, F. Liguori, P. Barbaro, S. Caporali, L. Merlo, C. Oldani, *ChemCatChem* **9** (2017) 4256–4267.
12. Y. Dou, M. Zhang, S. Zhou, C. Oldani, W. Fang and Q. Cao, *Eur. J. Inorg. Chem.*, **33** (2018) 3706–3716.
13. A. Karam, K. De Oliveira Vigier, S. Marinkovic, B. Estrine, C. Oldani, F. Jérôme, *ACS Catal.* **7** (2017) 2990–2997.
14. A. Karam, K. De Oliveira Vigier, S. Marinkovic, B. Estrine, C. Oldani, F. Jérôme, *ChemSusChem* **10** (2017) 3604–3610.
15. W. Fang, Z. Fan, H. Shi, S. Wang, W. Shen, H. Xu, J.-M. Clacens, F. De Campo, A. Liebens and M. Pera-Titus, *J. Mater. Chem. A* **4** (2016), 4380–4385.
16. A. Karam, A. Franco, M. Limousin, S. Marinkovic, B. Estrine, C. Oldani, K. De Oliveira Vigier, R. Luque, F. Jérôme *Catal. Sci. Technol.* **9** (2019) 1231-1237.
17. A. Corma, S. Iborra, A. Velty *Chem Rev* **107** (2007) 2411-2502.
18. D. Fan, D-J Dai, H-S Wu *Materials* **6** (2013) 101-115.
19. M. Zhung, Y. Yu, I & E C *Research* **52** (2013) 9505-9514.
20. A. Mohsenzadeh, A. Zumani, M.J. Taherzadeh *ChemBioEng Reviews* **4**(2) (2013) 75-90.
21. F. Cavani, S. Albonetti, F. Basile, A. Gandini, *Chemicals and Fuels from Bio-Based Building Blocks*, Wiley-VCH Verlag GmbH & Co. KGaA 2016.
22. C. Lucarelli, A. Lolli, A. Giugni, L. Grazia, S. Albonetti, D. Monticelli, A. Vaccari *Appl. Catal. B: Environmental* **203** (2017) 314-323.
23. C. Megías-Sayago, K. Chakarova, A. Penkova, A. Lolli, S. Ivanova, S. Albonetti, F. Cavani, J. A. Odriozola *ACS Catalysis* **8** (2018) 11154-11164.
24. G. Busca, *Chem. Rev.* **107** (2007) 5366-5410.
25. M. Pianca, E. Barchiesi, G. Esposto, S. Radice, *J. Fluorine Chem.*, **95** (1999) 71–84.
26. W. Fang, S. Wang, A. Liebens, F. De Campo, H. Xu, W. Shen, M. Pera-Titus, J. M. Clacens, *Catal. Sci. Technol.*, **5** (2015) 3980-3990.
27. S. H. De Almeida, Y. Kawano, *J. Therm. Anal. Calorim.*, **58** (1999) 569-577
28. L. Andrews, G. L. Johnson, *J. Chem. Phys.*, **79** (1983) 3670-3677.
29. C. A. Wilkie, J. R. Thomsen, M. L. Mittleman, *J. Appl. Polym. Sci.*, **42** (1991) 901-909.
30. S. R. Samms, S. Wasmus, R. F. Savinell, *J. Electrochem. Soc.*, **143** (1996) 1498-1504.
31. Q. Deng, C. A. Wilkie, R. B. Moore, K. Mauritz, *Polymer*, **39** (1998) 5961-5972.
32. A. Gruger, A. Regis, T. Schmatko, P. Colomban, *Vibr. Spectrosc.* **26** (2001) 215-225.
33. R. Tesser, M. Di Serio, L. Casale, L. Sannino, M. Ledda, E. Santacesaria *Chemical Engineering Journal* **161** (2010) 212–222.
34. N.G. Polyanskii, V.K. Sapozhnikov *Russ. Chem. Rev.*, **46** (1977) 445-476.
35. C. Park, M. A. Keane *J. Mol. Catal. A: Chemical* **166** (2001) 303–322
36. C. Reichardt, *Solvents and Solvent Effect in Organic Chemistry*, WILEY-VCH Verlag GmbH & Co. KGaA, Weinheim 2003.
37. M. A. Kader, A. K. Bhowmick, *Poly. Degrad. Stab.* **79** (2003) 283-295.
38. A. A. Zagorodni, *Ion Exchange Materials: Properties and Applications*, Elsevier, 2006.
39. A. Galadima, O. Muraza, *J. Ind. and Chem.* **31** (2015) 1-14.
40. T. T. Nguyen, V. Ruaux, L. Massin, C. Lorentz, P. Afanasiev, F. Maugè, V. Belliere-Baca, P. Rey, J. M. M. Millet, *Appl. Catal., B* **166-167** (2015) 432-444.
41. D. Varisli, T. Dogu, G. Dogu, *Chem. Eng. Sci.* **62** (2007) 5349-5352.
42. J. Sun, G. Yang, Y. Yoneyama, N.Tsubaki, *ACS Catal.* **4** (2014) 1078–1090.
43. K. Alexopoulos, M. John, K. Van der Borght, V. Galvita, M.-F. Reyniers, G. B. Marin, *J. Catal.*, **339** (2016) 173-185.

44. T. K. Phung, L. Proietti Hernández, A. Lagazzo, G. Busca, *Appl. Catal. A: Gen.* **493** (2015) 77–89.
45. T. K. Phung, G. Busca, *Chem. Eng. J.* **272** (2015) 92-101.
46. J. C. Soh, S. L. Chong, S. S. Hossain, C. K. Cheng *Fuel Process. Technol.* **158** (2017) 85-95.
47. N. Ozbay, N. Oktar, N. A Tapan, *Fuel* **87** (2008) 1789-1798.
48. Q. Sun. M. A. Harmer, W. E. Farneth, *Chem. Commun.*, (1996) 1201-1202.
49. P. F. Siril, A. D. Davison, J. K. Randhawa, D. R. Brown, *J. Mol. Catal. A: Chem.* **267** (2007) 72-78.